Applied Energy 123 (2014) 47–54

Contents lists available at ScienceDirect

Applied Energy

journal homepage: www.elsevier.com/locate/apenergy

The effect of temperature mismatch on thermoelectric generators electrically connected in series and parallel

Andrea Montecucco *, Jonathan Siviter, Andrew R. Knox

School of Engineering, College of Science and Engineering, University of Glasgow, UK

HIGHLIGHTS

- We study the electrical connection of thermoelectric generators (TEGs) in series and parallel arrays.
- We analyse the electrical characteristic of TEG arrays under mismatched temperature gradients.
- We experimentally quantify the power loss due to temperature mismatch in TEG arrays.
- We provide equations to estimate the electro-thermal effects that occur in each TEG within the series or parallel array.
- We discuss advantages and drawbacks of TEG arrays in series and parallel.

ARTICLE INFO

Article history:
Received 9 December 2013
Received in revised form 11 February 2014
Accepted 12 February 2014
Available online 12 March 2014

Keywords:
TEG
Mismatch
Series
Parallel
Peltier
Thermal imbalance

ABSTRACT

The use of thermoelectric generators (TEGs) to recover useful energy from waste heat has increased rapidly in recent years with applications ranging from microwatts to kilowatts. Several thermoelectric modules can be connected in series and/or parallel (forming an array) to provide the required voltage and/or current. In most TEG systems the individual thermoelectric modules are subject to temperature mismatch due to operating conditions. Variability of the electro-thermal performance and mechanical clamping pressure of individual TEG modules are also sufficient to cause a significant mismatch. Consequently, when in operation each TEG in the array will have a different electrical operating point at which maximum energy can be extracted and problems of decreased power output arise.

This work analyses the impact of thermal imbalance on the power produced at module and system level in a TEG array. Experimental results clearly illustrate the issue and a theoretical model is presented to quantify the impact. The authors believe the experimental results presented in this paper are the first to validate a rigorous examination of the impact of mismatched operating temperatures on the power output of an array of thermoelectric generators.

1. Introduction

Thermoelectric generators (TEGs) produce a current flow in an external circuit by the imposition of a temperature difference ΔT across the TEG. The magnitude of this ΔT determines the magnitude of the voltage difference ΔV and the direction of heat flow determines the voltage polarity.

The use of TEGs to recover waste heat energy has increased rapidly in recent years with applications in fields such as remote sensing [1–3], automotive [4–7], stove [8,9], geothermal [10], space systems [11] and industrial power plants [12–14]. Thermoelectrics are lately also combined to PV, solar thermal or thermophotovoltaic systems [15–17]. The power requirements depend strongly on the application, but span the range from microwatts to kilowatts. In systems where more than a few Watts are needed, several thermoelectric modules are deployed in arrays with series and/or parallel interconnections in order to provide the required power level. The method of interconnection of the TEGs is usually determined by the voltage and/or current required. The TEG can be electrically modelled as a voltage source in series with an internal resistance [18,19], as shown in Fig. 1. The values of both the voltage produced and the internal resistance vary with temperature.

The Peltier effect acts to pump heat from one side of the TEG to the other according to the current flowing through the device. As a consequence, the effective thermal resistance of the TEG depends to a certain extent on the magnitude of the current flowing in the external circuit [20,21]. In a thermoelectric generator the Peltier effect is considered to be parasitic and unwanted. Low electrical current will lead to a reduced thermal conductance

* Corresponding author. Tel.: +44 1413302180.
E-mail address: andrea.montecucco@glasgow.ac.uk (A. Montecucco).

http://dx.doi.org/10.1016/j.apenergy.2014.02.030
0306-2619

Nomenclature

ΔT	temperature difference (K)
V_{OC}	open-circuit voltage (V)
I_{SC}	short-circuit current (A)
R_{int}	internal resistance (Ω)
α	seebeck coefficient (μV/K)
a, b, c, d, e, f	constant coefficients independently calculated for each TEG
I_{load}	load current (A)
V_{load}	load voltage (V)

(high thermal resistance; low heat pumping), and high electrical current will lead to an increased thermal conductance (low thermal resistance; high heat pumping). If the TEG is electrically short circuited, the TEG will have the highest possible thermal conductance. This condition is normally avoided because it leads to a very inefficient thermal circuit with a large amount of heat energy being transferred from the 'hot' to the 'cold' side with no benefit in electrical power generation.

For a given thermal operating point the electrical power delivered by the TEG varies according to the current drawn by the electrical load. To maximise the power produced by the TEG, the electrical load impedance should equal the TEG's internal resistance (this is known as the "Maximum Power Transfer Theorem") [22,23]. The Maximum Power Point (MPP), the point at which the TEG delivers the maximum possible power to the external load for a given temperature) is given by half the open circuit voltage, $V_{OC}/2$, or by half of the short circuit current, $I_{SC}/2$.

Maximum power point tracking (MPPT) electronic converters are typically employed to maximise the power extracted [24]. This leads to the formation of what is called a distributed MPPT subsystem in which each TEG array's electrical operating point is controlled independently, in a similar way as for photovoltaic systems [25]. The primary motivation for this approach is that in most TEG systems the individual thermoelectric modules are subject to temperature mismatch. Examples of situations where this mismatch occurs directly include thermal variability as found in exhaust gas systems [6,26] or where the thermal conductivity of the mechanical system is poorly controlled [27]. Variability of the electro-thermal performance of individual TEG modules is also sufficient to cause a significant mismatch [28]. The mechanical clamping force the TEG is subjected to indirectly contributes to similar variation in electrical operating point, due to changes associated with the thermal contact resistance which is partially pressure dependent [29]. Consequently, when in operation each TEG in the array will have a different maximum power point. This maximum power point is the electrical operating point at which maximum energy can be extracted from the TEG. The normal operating condition for a TEG is to ensure that the load impedance is equal to (or greater) than the internal resistance, so that thermal conductance does not decrease the thermal to electrical conversion efficiency of the overall system. Ideally each TEG should be independently electronically controlled [30] but this would greatly increase the number and complexity of the MPPT power electronic converters needed and adversely affect the cost of implementing the system.

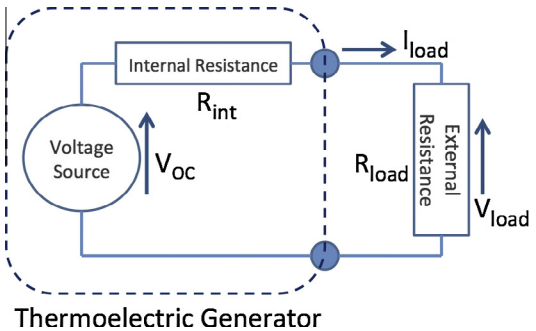

Fig. 1. Electrical model of a thermoelectric generator.

As the use of TEGs extends into progressively lower cost applications [31] the overall system economics dictate that a compromise must be found between the number of MPPT converters and the number of TEG modules connected to each converter. Problems of decreased thermal efficiency (due to parasitic Peltier effects) or decreased power output arise if the TEGs connected in the same array are subject to temperature mismatch because the MPPT converter sets the same suboptimal electrical operating point for each module in the array.

In the design of thermoelectric systems it is a key requirement to ensure that minimal temperature mismatch is applied to individual TEG devices. The aforementioned latest findings reported in the literature confirm that variable temperature distributions are commonly found in present thermoelectric systems. Some prototype systems show total performance lower than expected and sometimes thermoelectric system designers are not even aware of the effects of thermal imbalance.

However, no thorough analytical study has been undertaken to quantify the magnitude of this problem. Liang et al. [32] presented some experimental results for two TEGs electrically connected in parallel under different temperature but they focused only on showing how their theoretical model compared to real results. They did not quantify the power lost due to mismatched conditions out of the maximum power that the two TEGs would be producing if electrically loaded independently. The work we present in this article greatly extends this study and allows a quantitative assessment of the performance of interconnected TEG arrays when the elements are not all equally thermally heated. Also, the effect that non-optimal electrical operating points have on the thermal balance of each TEG is analysed.

The work presented in this article deals, for the first time in literature, with the issues related to thermally unbalanced TEGs connected in series and parallel, in a structured and rigorous way. It provides a way to predict the thermal and electrical behaviour of the system when several TEG devices are electrically connected in series or parallel, under balanced or unbalanced thermal conditions. Experimental results taken from an operating thermoelectric generating system using multiple thermally unbalanced TEGs confirm the theoretical analysis and provide a figure relative to the magnitude of power lost due to temperature mismatch. The results presented are discussed and a comparison between series and parallel connection of TEG arrays is provided, to assist in some design decisions related to thermoelectric systems. The experimental work we have conducted shows that simulation models [33] currently in use should be updated to include additional physical effects that were previously assumed not to have an impact.

2. Thermoelectric power generator device characteristic

The magnitude of the open-circuit TEG voltage is determined by the Seebeck coefficient and the magnitude of the absolute

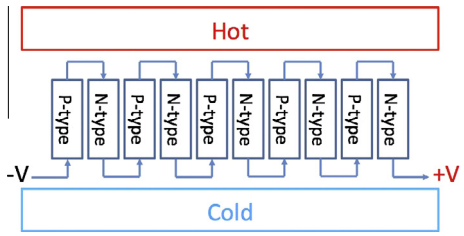

Fig. 2. Schematic diagram of thermoelectric couples in a thermoelectric device used as thermoelectric generator.

temperature. The *p*- and *n*-type semiconductors that make up a thermoelectric device are arranged in series electrically, and in parallel thermally, as shown in Fig. 2. The voltage from each element is added such that a device comprising many such elements produces a usable voltage. Each *p*- and *n*-pair is referred to as thermocouple.

The magnitude of the voltage also depends on the materials in use, and different materials may be optimised for different temperature regions [34–37]. A typical Bismuth Telluride (Bi_2Te_3) thermocouple has a Seebeck coefficient of around 350 μV/K. In a larger device there are typically 127, 254 or 449 pairs that can achieve open circuit voltages over 30 V at high ΔT.

In operation, the TEG will be subject to a range of thermal and mechanical stresses and these stresses limit the physical size of the TEG module to typically less than 100×100 mm^2. The stresses induced in the module are in part a consequence of the variation in the physical size of the top and bottom layers enclosing the pellets of the thermoelectric material, and the variation in size is a consequence of the mismatch in the thermal expansion or contraction of the materials used to construct the TEG. The semiconductor material directly changes the thermal conductivity of the material which in turn affects the slope of the thermal gradient and adds to the mechanical stresses experienced during the operation.

Fig. 3 shows the performance curve for a thermoelectric module (product code: *GM250-449-10-12* by *European Thermodynamics Ltd.*) formed of 449 couples with a physical size of 55×55 mm^2 when operated at a ΔT of 220 °C. The blue straight line represents the voltage versus current (*V–I*) characteristic, while the red curved line is the power curve (*P–I*) for the device. The open-circuit voltage V_{OC} is the voltage when no current is drawn by the load, while the short-circuit current I_{SC} is the current when the TEG's terminals are shorted together. The maximum power point lies at the point when $I_{load} = I_{SC}/2$ or $V_{load} = V_{OC}/2$ and is established when the equivalent electrical load resistance in the external circuit connected to the TEG exactly equals the internal electrical resistance R_{int} of the TEG. R_{int} is the inverse slope of the *V–I* line and its absolute value is dependent on the temperature at which the TEG is operating and hence does not have a fixed value. When the TEG is operated to the left of the maximum power point as shown in Fig. 3, reduced current flows through the TEG and the effective thermal conductivity of the TEG (which depends also on the current flow, due to the parasitic Peltier effect) decreases. Under this condition the thermal energy conducted via the TEG is less than that at the maximum power point and hence a lower thermal load is imposed on the overall system. This is advantageous in most circumstances since it leads to increased thermal efficiency of the system. When the TEG is operated to the right of the maximum power point then the thermal conductivity increases and the thermal energy conducted via the TEG is greater than that which flows at the maximum power point. Operation in the region to the right on Fig. 3 leads to a reduced thermal efficiency of the system. For the module data shown in Fig. 3, the maximum power is approximately 13.2 W with a corresponding output voltage of 16.5 V (being half of the open-circuit voltage of 33 V).

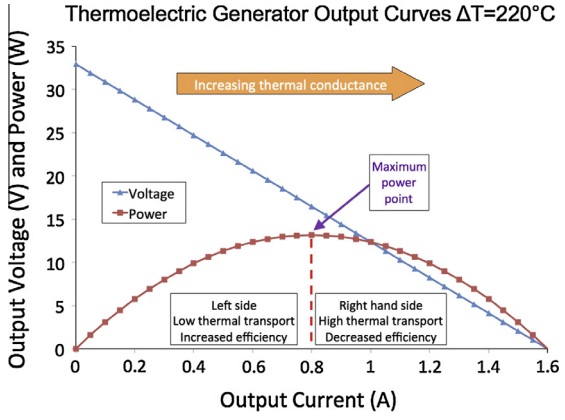

Fig. 3. Electrical characterisation (*V–I* and *P–I* curves) of the thermoelectric generator *GM250-449-10-12* by *European Thermodynamics Ltd.*

3. Series and parallel array configurations

In practical thermoelectric systems, several thermoelectric modules are often deployed in arrays with series and/or parallel interconnections in order to achieve larger values of current and voltage. The method of interconnection of the TEGs is usually determined by the voltage and/or current required.

3.1. Series array configuration

Fig. 4 illustrates the series connection of three TEGs, each of them represented by a voltage source $V_{1,\ldots,3}$ in series with an internal resistance $R_{1,\ldots,3}$.

Under ideal operating conditions, each module within the array will experience an equal ΔT and therefore all modules will produce an equal output voltage V_{OC} and the array will be in a balanced thermal condition. In this case the MPP is at $3V_{OC}/2$ and the overall array resistance is $3R_{int}$.

However, actual thermal operating conditions in a practical system might be such that each TEG may experience a different ΔT and therefore their voltages and internal resistances will not be equal. In this case $V_{OC} = V_1 + V_2 + V_3$ and the current flowing into the load is

$$I = \frac{V_{OC} - V_S}{R_1 + R_2 + R_3} \tag{1}$$

where V_S is the voltage at the array's terminals.

3.2. Parallel array configuration

Fig. 5 shows three TEGs in a parallel configuration. For ideal operating conditions, the TEG modules in the array operate at the same ΔT. Hence each TEG produces the same voltage and operates at maximum power, with $I_1 = I_2 = I_3$.

Under non-ideal thermal conditions the different temperature gradient across each TEG unit will lead to a mismatch in the currents magnitude:

$$I_1 = \frac{V_1 - V_P}{R_1} \qquad I_2 = \frac{V_2 - V_P}{R_2}$$
$$I_3 = -I_1 - I_2 \tag{2}$$

where V_P is the voltage at the arrays terminals.

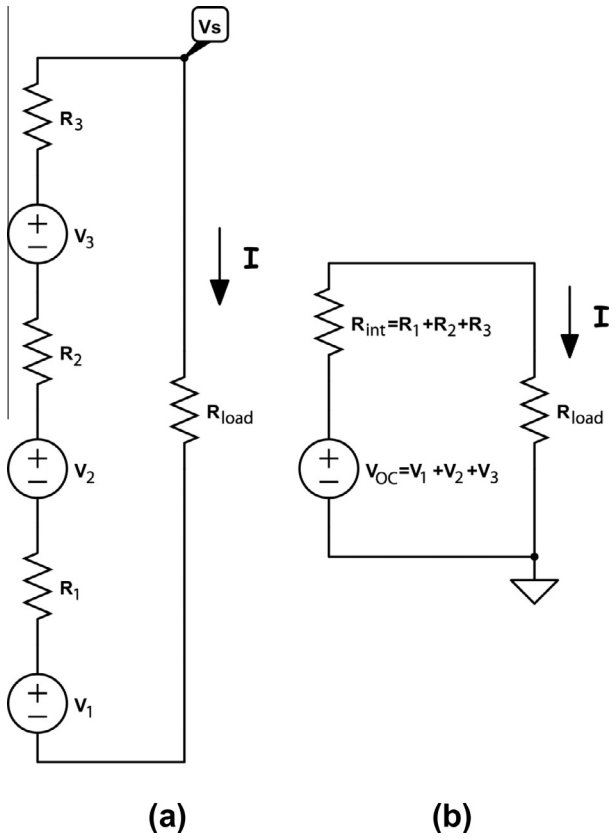

Fig. 4. Electrical schematic of an array of three TEG modules electrically connected in series (left) and its equivalent representation (right).

4. Experimental setup

In order to characterise the performance of the thermoelectric devices in multiple connection configurations and with different temperature gradients, the measurement system presented in [29] has been used.

This test apparatus provides accurate and repeatable measurements and is able to independently control the mechanical load and the temperature difference across each of the four TEG channels that can be used at the same time. Fig. 6 illustrates the schematic of one channel. The TEG device is sandwiched between a hot block and a cold block. The former contains a high-temperature high-power heater powered by a DC power supply, while the latter is water-cooled by a chiller unit. The output of the TEG can be connected to an electronic load or to any other desired load. A load cell measures the mechanical pressure over the TEG and thermocouple sensors are fitted through the copper blocks touching the TEGs' hot and cold faces, in order to obtain precise temperature measurements. A data logger unit is used to record temperature and mechanical pressure measurements from the test fixture and all the instruments are fully programmable and operated from a laptop PC running an *Agilent* VEE Pro program. VEE Pro is a graphical programming tool for automated control of laboratory equipment. Maintaining the temperature difference across the thermoelectric device to the desired value it is possible to obtain an accurate electrical characterisation of the TEG under test, sweeping the load at different values, all at the same temperature difference.

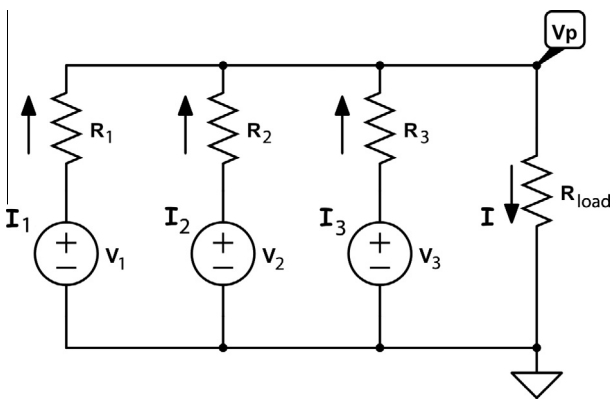

Fig. 5. Electrical schematic of an array of three TEG modules electrically connected in parallel.

All the data provided was obtained using three identical TEG devices by *European Thermodynamics Ltd.* (product code: *GM250-127-14-10*). Every test was performed imposing 1.25 *MPa* of mechanical pressure onto each TEG, which corresponds to 200 kg on a surface of 40×40 mm^2.

4.1. Individual TEG characterisation

The individual electrical characteristic of each of the three TEGs is achieved at three different thermal operating points: $\Delta T = 100\,^{\circ}$C,150 °C and 200 °C. Fig. 7 shows the resulting performance curves for TEG# 2.

Table 1 lists the performance data of the three TEGs, together with the maximum deviation between the three devices, which stands at less than 5% for what concerns power production.

Next, using a similar technique to that explained in [38], a mathematical characterisation has been developed in order to be able to calculate any voltage and power as a function of the current load and temperature difference. Referring to Fig. 1, it can be written that

$$V_{load} = V_{OC} - R_{int} I_{load} \tag{3}$$

The open-circuit voltage is proportional to the Seebeck coefficient $\alpha (V_{OC} = \alpha T)$, which is not constant but varies depending on the Thomson coefficient [39]. In order to account for the variation of V_{OC} and R_{int} with ΔT, a 2nd-order polynomial curve fitting technique has been used, as shown in Fig. 8 for TEG# 2. Hence the Eq. (3) can be now written as

$$V_{load} = (a\Delta T^2 + b\Delta T + c) - (d\Delta T^2 + e\Delta T + f) I_{load} \tag{4}$$

where a, b, c, d, e and f are constant coefficients, different for each TEG. Table 2 lists the $a, \ldots, f$ parameters for the three TEGs used in the experiments. If a TEG producing half the voltage and double the amount of current was to be used, then the coefficients a, b, c would need to be halved and d, e, f divided by 4.

Using Eq. (4) it is possible to replicate the electrical characteristics of the TEGs used, after obtaining the necessary parameters from the experimental data. Fig. 9 shows the resulting 'mathematical' electrical characterisation for TEG# 2. As it can also be appreciated from a comparison with Fig. 7, the average deviation between the mathematically derived values and the experimental data is always less than 1.5%. This means that it is now possible to independently predict the output from each of the three TEGs with high confidence, even when they are at different thermal operating points.

5. Experimental results

This section presents the experimental electrical characterisations of arrays of TEGs connected in series and parallel while subject to temperature mismatch. For each configuration a theoretical

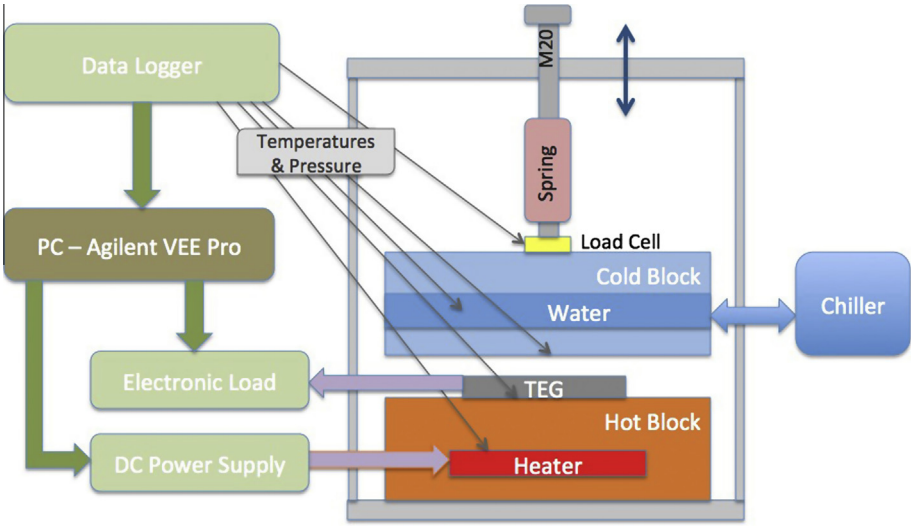

Fig. 6. Schematic of the mechanical test rig used in the experiments.

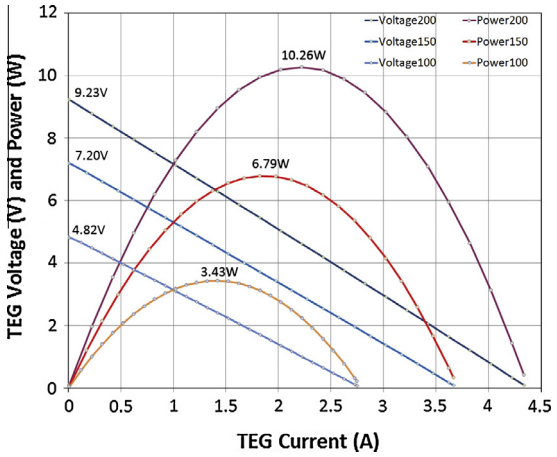

Fig. 7. Experimental electrical characterisation for the TEG module # 2. The grey dots in the curves represent experimental data points. $\Delta T = 100\,^{\circ}C$, 150 °C, 200 °C, clamped at 2 kN/1.25 MPa.

analysis is presented to explain behaviour during the open-circuit condition and to predict the at-load maximum power point and associated thermal behaviour.

5.1. Series array configuration

The three TEGs were connected electrically in series into an array whose electrical characterisation was performed with TEG# 1 at 100 °C, TEG# 2 at 150 °C and TEG# 3 at 200 °C. The results obtained from the array of TEGs are shown in Fig. 10.

The maximum power that can be extracted (18.22 W) is less than the sum of powers that could be produced by the array if the TEGs were individually connected. From Table 1 this value can be calculated as 3.43 W(TEG# 1) + 6.8 W(TEG# 2)+ 9.84 W(TEG# 3) = 20.07 W. This means that when under the selected temperature-mismatched condition the three thermoelectric devices produced 9.22% less power. It must be noted that the wiring and connectors used for the series connection of the TEGs contribute to additional electrical resistance which in turns decreases the total output power from the TEG array.

It can be noted that the MPP is found when the array's terminals voltage is at half of the open-circuit value. This result confirms the fact that an array of TEGs in series can be simplified to a voltage source, whose value is the sum of the individual TEGs' open-circuit voltages (from Table 1, $4.84V + 7.23V + 9.2V = 21.27V$), and an internal resistance equal to the sum of the individual internal resistances, as already described in Section 3.1. This confirms that a MPPT converter using the fractional open-circuit voltage method is still able to obtain the MPP of a mismatched array.

It is of great interest to understand the operating point for each module relative to its *V–I* curve, while series-connected in the (mismatched) array. The current is the same in each TEG and, from Fig. 10, is found to be 1.72 A. Reference to Fig. 7 shows that TEG# 1 (100 °C) is working on the right-hand side of its power *P–I* curve (orange coloured); this means that it is working on a less efficient thermal operating point with higher Peltier effect (hence higher effective thermal conductivity) which leads to a decrease in temperature difference across it, thus amplifying the mismatched condition. TEG# 2 (150 °C) works very close to its MPP, while TEG# 3 (200 °C) works on the left-hand side of its power curve (in purple); this corresponds to working in a more efficient operating point which leads to an increase in the temperature gradient across it.

Table 1
Performance parameters for the three thermoelectric modules used in the experiment.

ΔT (°C)	TEG# 1			TEG# 2			TEG# 3			Deviation		
	R_{int} (Ω)	V_{OC} (V)	P_{max} (W)	R_{int} (Ω)	V_{OC} (V)	P_{max} (W)	R_{int} (Ω)	V_{OC} (V)	P_{max} (W)	R_{int} (%)	V_{OC} (%)	P_{max} (%)
100	1.73	4.84	3.43	1.73	4.87	3.44	1.80	4.87	3.33	3.8	0.7	3.2
150	1.94	7.22	6.79	1.94	7.23	6.80	2.01	7.21	6.57	3.6	0.2	3.4
200	2.11	9.25	10.26	2.10	9.25	10.30	2.17	9.20	9.84	3.3	0.5	4.5

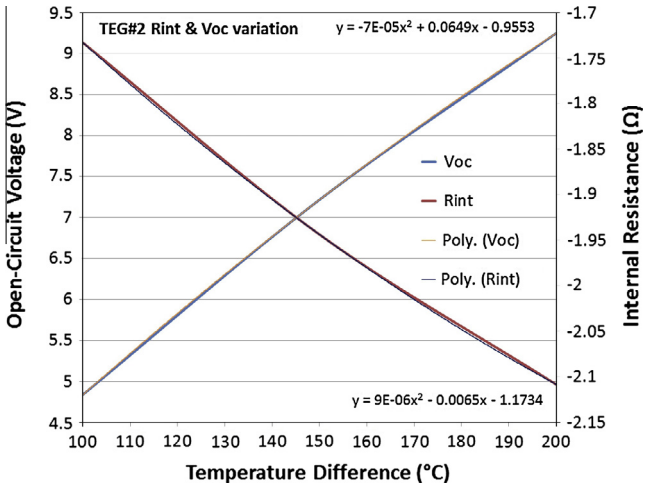

Fig. 8. Variation of the open-circuit voltage and the internal resistance of TEG# 2 with the temperature difference. 2nd-order polynomial fitting has been used to express the variation mathematically.

Table 2
a, b, c, d, e, f Coefficients for the three TEGs used in the experiments.

	V_{OC} (V)			R_{int} (Ω)		
	a (V/K^2)	b (V/K)	c (V)	d (Ω/K^2)	e (Ω/K)	f (Ω)
TEG# 1	$-7 \cdot 10^{-5}$	0.0649	−0.9553	$-9 \cdot 10^{-6}$	0.0065	1.1734
TEG# 2	$-7 \cdot 10^{-5}$	0.0639	−0.8536	$-9 \cdot 10^{-6}$	0.0062	1.1972
TEG# 3	$-7 \cdot 10^{-5}$	0.064	−0.8369	$-1 \cdot 10^{-5}$	0.0067	1.2328

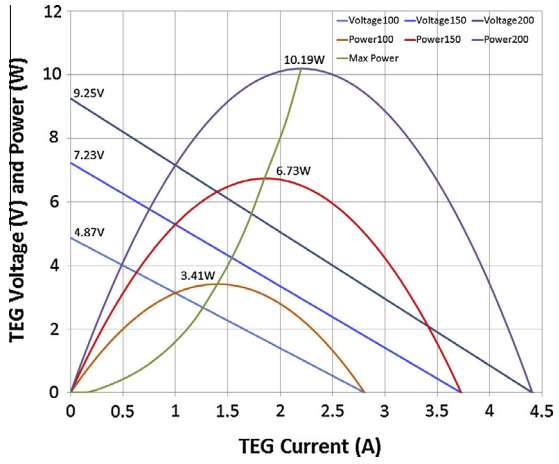

Fig. 9. 'Mathematical' electrical characterisation for the TEG module # 2.

This results in a positive feedback effect for which, in the case where the input power source remains constant, the temperature mismatch is greater.

5.2. Parallel array configuration

The three TEGs were connected electrically in parallel into an array whose electrical characterisation was performed with TEG# 1 at 100 °C, TEG# 2 at 150 °C and TEG# 3 at 200 °C. The results are shown in Fig. 11.

Confirming that the MPP is still at half of V_{OC}, Fig. 11 shows that the available maximum power is now 17.48 W, which is 12.90% less than what would be available if each TEG was to be controlled

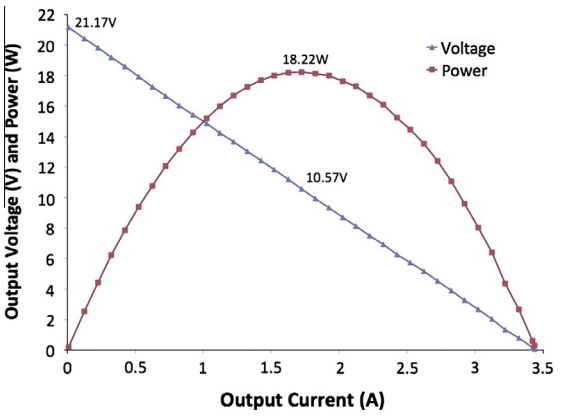

Fig. 10. Electrical characterisation of an array with three TEGs in series under mismatched temperature difference: $\Delta T_{TEG\#\ 1} = 100$ °C; $\Delta T_{TEG\#\ 2} = 150$ °C; $\Delta T_{TEG\#\ 3} = 200$ °C.

individually. This is also less than the electrically-in-series case. The additional wire and connectors used are responsible for part of this power lost, however the comparison of performance between series and parallel case remains valid because of the same number of connections used.

Predicting the open-circuit voltage of an array with mismatched TEGs connected in parallel is not as straightforward as when the TEGs are connected in series, because the value depends on the individual TEGs' voltages and internal resistances. Looking at the circuit in Fig. 5, when R_{load} is not connected the sum of currents at node V_P is null (Eq. (2) remains true). Each current can be written as

$$I_n = \frac{V_n - V_P}{R_n} \tag{5}$$

where $n = 1, \ldots, 3$. Substituting Eq. (5) (for each module) into Eq. (2) it is now possible to obtain V_P:

$$V_P = \frac{R_2R_3V_1 + R_1R_3V_2 + R_1R_2V_3}{R_1R_2 + R_1R_3 + R_2R_3} \tag{6}$$

Depending on the value of V_P the value of each TEGs current may be positive or negative. A positive value of current means that the module, while the array is in open-circuit, i.e. no external load is applied, is generating current; on the contrary a negative value of current means that the module is absorbing current, hence working in heat pumping mode. The values of currents in the situation chosen for the experiment are not irrelevant, as it will be now calculated and measured. Using the mathematical technique described in Section 4.1 (Eq. (4)) the current in each TEG were found to be:

$$I_1 = 1.19\ \text{A}, \quad I_2 = -0.14\ \text{A}, \quad I_3 = -1.05\ \text{A} \tag{7}$$

These values were then confirmed by a transient experiment: the three TEGs, disconnected from each other, were first brought to the selected temperature gradients ($\Delta T_{TEG\#\ 1} = 100$ °C; $\Delta T_{TEG\#\ 2} = 150$ °C; $\Delta T_{TEG\#\ 3} = 200$ °C), then instantaneously connected in parallel through two multimeters in current mode, as depicted in Fig. 12. The current going from TEG# 3 to TEG# 2, I_{32}, was 0.95 A while the current going from TEG# 2 to TEG# 1, I_{21}, was 1.10 A. The difference with the results of Eq. (7) stands around 10%, which can be attributed to the difficulty in reading the multimeter during the transient, to the frequency response of the multimeter itself and to the thermal effects occurring during the transient from open-circuit to short-circuit.

As in the previous procedure for the series array, it is relevant to establish the operating point of each TEG with reference to its P-I curve. In this case of parallel electrical connection of the modules

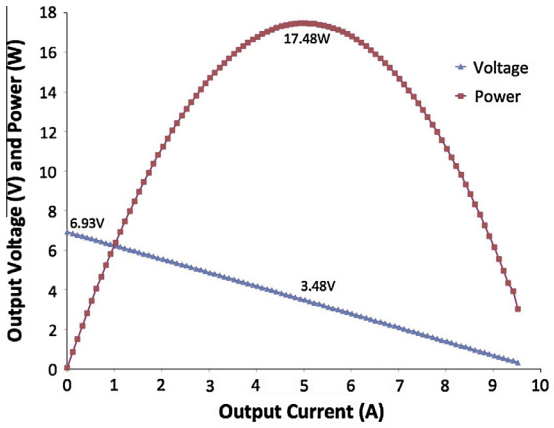

Fig. 11. Electrical characterisation of an array with three TEGs in parallel under mismatched temperature difference: $\Delta T_{TEG\#\ 1} = 100\ ^\circ C$; $\Delta T_{TEG\#\ 2} = 150\ ^\circ C$; $\Delta T_{TEG\#\ 3} = 200\ ^\circ C$.

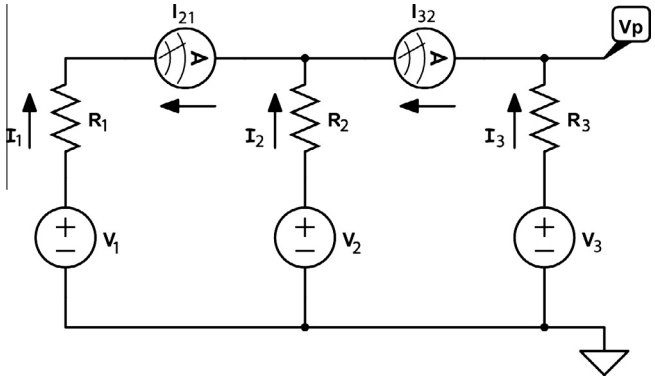

Fig. 12. Equivalent circuit diagram of the experimental setup used to measure the instantaneous current flowing after the sudden parallel connection of mismatched thermoelectric devices.

the operating voltage is the same for each TEG (3.48 V). TEG# 1 (100 °C) works on the left-hand side of its power *P–I* curve (orange coloured), which corresponds to a higher efficiency point which tends to increase its temperature difference. TEG# 2 (150 °C) works very close to its MPP, and TEG# 3 (200 °C) works on the right-hand side of its power curve (purple-coloured), where the Peltier effect is greater, leading to a decrease in temperature difference across it. The overall effect can be described as a negative feedback, for which the TEGs operating at lower and higher temperature gradients, i.e. TEG# 1 and TEG# 3 respectively, are pushed towards the middle temperature difference of TEG# 2.

5.3. Discussion of results

The presented results convey the idea that connecting thermoelectric generators in series produces better electrical system efficiency, provided that the temperature differences remain constant. The temperature-mismatch situation created in the experiment demonstrated a power production drop of 9.22% and 12.90%, for the series and parallel case respectively, from the maximum power that would be available in case each TEG was controlled individually. Part of this power lost is due to the wiring and connectors used for the array interconnections.

However, from the thermal point of view the parallel connection showed that its thermal equalising influence would bring all the TEGs' temperature differences towards a value in the middle, if the thermal input powers to the TEGs remain constant. This would decrease the temperature mismatch and increase the array electrical efficiency. At the same time, reducing the temperature gradient across the TEG at highest temperature difference could prove unwanted because output power increases exponentially with temperature difference. This situation has not been studied in this work and will be researched in the future to better understand its advantages and disadvantages.

From the electrical connection point of view, the parallel-connected array has lower voltage and higher current, which leads to higher I^2R losses (Joule heating) in the wiring and MPPT converter, thus further decreasing the overall system electrical efficiency. System cost in parallel connection is adversely affected because of the need for high-current inductors in the Switch-Mode Power Supplies (SMPS), and possibly more complicated SMPS topologies in case that high-step up is required. Especially in low-temperature applications a higher open-circuit voltage is preferred because it calls for a simpler and more efficient power converter.

When designing a thermoelectric generating system a balance must be found between the number of MPPT converters and the number of TEGs connected into an array controlled by one of those power converters. This work ultimately suggests that the connection of thermoelectric devices in series yields a more efficient system at lower cost, compared to parallel connection. This is true considering both non-uniform temperature distributions, as researched in this paper, and the aforementioned considerations related to Joule losses and size and cost of wiring and electronic components.

Future work will investigate solutions to diminish the negative impact of thermo-mechanic mismatches on the thermal and electrical efficiency of interconnected TEG arrays.

6. Conclusion

This work describes the electro-thermal effects occurring in arrays of thermoelectric generators connected in series and in parallel, when the individual devices are exposed to non-uniform temperature gradients. Experimental data are presented to show that such problem can impact the performance of a thermoelectric system, and a theoretical analysis is presented to justify the results and to calculate expected performance. The experimental results show that the power lost by mismatched conditions (temperature, mechanical load, manufacturing tolerances, aging) can be significant, and it is lower in the series connected array.

This work provided both a mathematical formulation (achievable from experimental characterisation) and electrical circuit equations that together can be used to predict the output electrical power in any temperature mismatch situation. This work analysed arrays of three TEGs, however the results and the circuit equations can easily be adapted for a higher number of TEGs.

In commercial systems that are currently under development for energy scavenging from vehicle exhaust gases there are arrays which are subject to different temperatures. There is a need for multiple power converters, however this is insufficient to guarantee that the maximum possible power will actually be achieved. Simulation models currently in use should be updated to include the additional physical effects due to temperature imbalance, otherwise risking to over-estimate total power production.

The presented results suggest that series electrical connection enables more of the available power to be captured and that Joule heating losses in wiring and the electronics are minimised. In the practical case where thermal–mechanical imbalances may be expected, a balance must be found between the number and cost of MPPT converters in a distributed system, and the expected power loss due to mismatched conditions.

Acknowledgement

The authors would like to thank Mr. Peter Miller for his support in creating the test rig used for the experiments. This work has been partially funded by the EPSRC grant EP/K022156/1 (RCUK).

References

[1] Ferrari M, Ferrari V, Guizzetti M, Marioli D, Taroni A. Characterization of thermoelectric modules for powering autonomous sensors. In: Instrumentation and Measurement Technology Conference (IMTC) 2007. p. 1–6.
[2] Yu H, Li Y, Shang Y, Su B. Design and investigation of photovoltaic and thermoelectric hybrid power source for wireless sensor networks. In: 3rd IEEE int. conf. on nano/microengineered and molecular systems 2008. p. 196–201.
[3] Wang W, Cionca V, Wang N, Hayes M, O'Flynn B, O'Mathuna C. Thermoelectric energy harvesting for building energy management wireless sensor networks. Int J Distrib Sens Networks 2013.
[4] Haidar J, Ghojel J. Waste heat recovery from the exhaust of low-power diesel engine using thermoelectric generators. In: 20th International Conference on Thermoelectrics (ICT'01); 2001. p. 413–8.
[5] Anatychuk LI, Kuz RV, Rozver YY. Efficiency of thermoelectric recuperators of the exhaust gas energy of internal combustion engines. In: 9th European Conference on Thermoelectrics (ECT'11) 2011. p. 516–9.
[6] Crane D, LaGrandeur J, Jovovic V, Ranalli M, Adldinger M, Poliquin E, et al. TEG on-vehicle performance and model validation and what it means for further TEG development. J Electron Mater 2012.
[7] Risse S, Zellbeck H. Close-coupled exhaust gas energy recovery in a gasoline engine. Res Therm Manage 2013;74:54–61.
[8] Champier D, Bedecarrats JP, Kousksou T, Rivaletto M, Strub F, Pignolet P. Study of a TE (thermoelectric) generator incorporated in a multifunction wood stove. Energy 2011;36:1518–26.
[9] O'Shaughnessy S, Deasy M, Kinsella C, Doyle J, Robinson A. Small scale electricity generation from a portable biomass cookstove: prototype design and preliminary results. Appl Energy 2013;102:374–85.
[10] Suter C, Jovanovic Z, Steinfeld A. A 1 kWe thermoelectric stack for geothermal power generation – modeling and geometrical optimization. Appl Energy 2012;99:379–85.
[11] Rowe D. Thermoelectric waste heat recovery as a renewable energy source. Int J Innovations Energy Syst Power 2006;1:13–23.
[12] Furue T, Hayashida T, Imaizumi Y, Inoue T, Nagao K, Nagai A, Fujii I, Sakurai T. Case study on thermoelectric generation system utilizing the exhaust gas of interal-combustion power plant. In: 17th International Conference on Thermoelectrics (ICT'98). 1998. p. 473–8.
[13] Kaibe H, Makino K, Kajihara T, Fujimoto S, Hachiuma H. Thermoelectric generating system attached to a carburizing furnace at Komatsu Ltd., Awazu Plant. In: 9th European Conference on Thermoelectrics (ECT'11) 2011. p. 524–7.
[14] Siviter J, Knox A, Buckle J, Montecucco A, Euan M. Megawatt scale energy recovery in the Rankine cycle. In: IEEE Energy Conversion Congress and Exposition (ECCE'12) 2012. p. 1374–9.
[15] Sark WV. Feasibility of photovoltaic thermoelectric hybrid modules. Appl Energy 2011;88:2785–90.
[16] Xiao J, Yang T, Li P, Zhai P, Zhang Q. Thermal design and management for performance optimization of solar thermoelectric generator. Appl Energy 2012;93:33–8.
[17] Qiu K, Hayden aCS. Development of a novel cascading TPV and TE power generation system. Appl Energy 2012;91:304–8.
[18] Rowe D, Min G. Evaluation of thermoelectric modules for power generation. J Power Sources 1998;73:193–8.
[19] Lineykin S, Ben-Yaakov S. Modeling and analysis of thermoelectric modules. IEEE Trans Ind Appl 2007;43:505–12.
[20] Montecucco A, Buckle JR, Knox AR. Solution to the 1-D unsteady heat conduction equation with internal Joule heat generation for thermoelectric devices. Appl Therm Eng 2012;35:177–84.
[21] Kim S. Analysis and modeling of effective temperature differences and electrical parameters of thermoelectric generators. Appl Energy 2013;102:1458–63.
[22] Laird I, Lovatt H, Savvides N, Lu D, Agelidis VG. Comparative study of maximum power point tracking algorithms for thermoelectric generators. In: Australasian Universities Power Engineering Conference (AUPEC'08), 2008.
[23] Montecucco A, Siviter J, Knox AR. Simple, fast and accurate maximum power point tracking converter for thermoelectric generators. In: IEEE Energy Conversion Congress and Exposition (ECCE'12) 2012. p. 2777–83.
[24] Laird I, Lu DD-C. High step-up DC/DC topology and MPPT algorithm for use with a thermoelectric generator. IEEE Trans Power Electron 2013;28:3147–57.
[25] Pilawa-Podgurski RCN, Perreault DJ. Submodule integrated distributed maximum power point tracking for solar photovoltaic applications. IEEE Trans Power Electron 2013;28:2957–67.
[26] Wang Y, Dai C, Wang S. Theoretical analysis of a thermoelectric generator using exhaust gas of vehicles as heat source. Appl Energy 2013;112:1171–80.
[27] Lee H. Optimal design of thermoelectric devices with dimensional analysis. Appl Energy 2013;106:79–88.
[28] Hatzikraniotis E, Zorbas KT, Samaras I, Kyratsi T, Paraskevopoulos KM. Efficiency study of a commercial thermoelectric power generator (TEG) under thermal cycling. J Electron Mater 2009;39:2112–6.
[29] Montecucco A, Buckle J, Siviter J, Knox AR. A new test rig for accurate nonparametric measurement and characterization of thermoelectric generators. J Electron Mater 2013.
[30] Wu H, Sun K, Chen M, Chen Z, Xing Y. Hybrid centralized-distributed power conditioning system for thermoelectric generator with high energy efficiency. In: IEEE Energy Conversion Congress and Exposition (ECCE'13) 2013. p. 4659–64.
[31] Patyk A. Thermoelectric generators for efficiency improvement of power generation by motor generators environmental and economic perspectives. Appl Energy 2013;102:1448–57.
[32] Liang G, Zhou J, Huang X. Analytical model of parallel thermoelectric generator. Appl Energy 2011;88:5193–9.
[33] Montecucco A, Knox AR. Accurate simulation of thermoelectric power generating systems. Appl Energy 2014;118:166–72.
[34] Samarelli A, Ferre Llin L, Cecchi S, Frigerio J, Etzelstorfer T, Muller E, et al. The thermoelectric properties of Ge/SiGe modulation doped superlattices. J Appl Phys 2013;113:233704.
[35] Brignone M, Ziggiotti A. Impact of novel thermoelectric materials on automotive applications. In: 9th European Conference on Thermoelectrics (ECT'11) 2011. p. 493–6.
[36] Fergus JW. Oxide materials for high temperature thermoelectric energy conversion. J Eur Ceram Soc 2012;32:525–40.
[37] Ferre Llin L, Samarelli A, Cecchi S, Etzelstorfer T, Muller Gubler E, Chrastina D, et al. The cross-plane thermoelectric properties of p-Ge/Si0.5Ge0.5 superlattices. Appl Phys Lett 2013;103:143507.
[38] Woo BC, Lee DY, Lee HW, Kim IJ. Characteristic of maximum power with temperature difference for thermoelectric generator. In: 20th International Conference on Thermoelectrics (ICT'01); 2001. p. 431–4.
[39] Chen J, Yan Z, Wu L. The influence of Thomson effect on the maximum power output and maximum efficiency of a thermoelectric generator. J Appl Phys 1996;79:8823.